Clinical Neurophysiology 127 (2016) 3165–3175

Contents lists available at ScienceDirect

Clinical Neurophysiology

journal homepage: www.elsevier.com/locate/clinph

# Graph analysis of EEG resting state functional networks in dyslexic readers

G. Fraga González [a,*], M.J.W. Van der Molen [b,c], G. Žarić [d], M. Bonte [d], J. Tijms [a,e], L. Blomert [d,✠], C.J. Stam [f], M.W. Van der Molen [a,g]

[a] Department of Psychology, University of Amsterdam, The Netherlands
[b] Leiden University, Institute of Psychology, The Netherlands
[c] Leiden Institute for Brain and Cognition, Leiden University, The Netherlands
[d] Department of Cognitive Neuroscience, Faculty of Psychology and Neuroscience, University of Maastricht, The Netherlands
[e] IWAL Institute, Amsterdam, The Netherlands
[f] Department of Clinical Neuropsychology and MEG Center, Neuroscience Campus Amsterdam, VU University Medical Center, Amsterdam, The Netherlands
[g] Amsterdam Brain and Cognition, University of Amsterdam, The Netherlands

ARTICLE INFO

*Article history:*
Accepted 8 June 2016
Available online 4 July 2016

*Keywords:*
Electroencephalography (EEG)
Functional connectivity
Network
Graph theory
Minimum spanning tree
Dyslexia

HIGHLIGHTS

- Organization of brain networks in dyslexics and typically-reading controls.
- Minimum spanning tree (MST) graphs were derived from connectivity matrices.
- Graph metrics in the theta-band showed less integrated network configuration in dyslexics.

ABSTRACT

*Objective:* Neuroimaging research suggested a mixed pattern of functional connectivity abnormalities in developmental dyslexia. We examined differences in the topological properties of functional networks between 29 dyslexics and 15 typically reading controls in 3rd grade using graph analysis. Graph metrics characterize brain networks in terms of integration and segregation.
*Method:* We used EEG resting-state data and calculated weighted connectivity matrices for multiple frequency bands using the phase lag index (PLI). From the connectivity matrices we derived minimum spanning tree (MST) graphs representing the sub-networks with maximum connectivity. Statistical analyses were performed on graph-derived metrics as well as on the averaged PLI connectivity values.
*Results:* We found group differences in the theta band for two graph metrics suggesting reduced network integration and communication between network nodes in dyslexics compared to controls.
*Conclusion:* Collectively, our findings point to a less efficient network configuration in dyslexics relative to the more proficient configuration in the control group.
*Significance:* Graph metrics relate to the intrinsic organization of functional brain networks. These metrics provide additional insights on the cognitive deficits underlying dyslexia and, thus, may advance our knowledge on reading development. Our findings add to the growing body literature suggesting compromised networks rather than specific dysfunctional brain regions in dyslexia.


## 1. Introduction

Reading involves integrated functioning of complex brain networks. Distinct brain systems, mostly in the left hemisphere, have been proposed to specialize during reading acquisition (see a review in Schlaggar and McCandliss, 2007). Studies in developmental dyslexia revealed various disturbances of the brain networks implicated in reading. Studies using diffusion tensor

* Corresponding author at: Department of Psychology, University of Amsterdam, Nieuwe Achtergracht 129B, 1018 WS Amsterdam, The Netherlands.
*E-mail address:* G.FragaGonzalez@uva.nl (G. Fraga González).
✠ Leo Blomert passed away on November 25, 2012.

http://dx.doi.org/10.1016/j.clinph.2016.06.023
1388-2457/

imaging (DTI) to examine white matter properties of the main pathways that constitute the anatomical basis of the network reported reduced connectivity in dyslexia (for a review and meta-analysis Vandermosten et al., 2012). Similarly, a score of functional magnetic resonance imaging (fMRI) studies in adults reported reduced connectivity of the reading network (e.g., Pugh et al., 2000; Quaglino et al., 2008; Schurz et al., 2014; Shaywitz et al., 2003; Stanberry et al., 2006; Van der Mark et al., 2011; but see Richards and Berninger, 2008) and other connectivity disturbances (Finn et al., 2014; Wolf et al., 2010). A recent MRI study examining the topological organization in Chinese dyslexic children revealed a less integrated network organization relative to typically reading controls, characterized by increased local processing and less long-range communication (Liu et al., 2015).

The neural network studies highlight the interactive nature of brain systems implicated in reading and underscore the relevance of connectivity to the study of dyslexia. Although specific brain regions have been successfully linked to literacy acquisition, the understanding of a highly complex cognitive function such as reading may also require a more integrative and holistic view of brain function, which can be conceptualized as a complex network (Bullmore and Sporns, 2009). In relation to this, previous neuroimaging research showed that examining the dynamics of spontaneous (task independent) activity in the brain provide us with meaningful information about how different brain areas communicate (van den Heuvel and Hulshoff Pol, 2010) and the underlying architecture of functional brain networks (Gusnard and Raichle, 2001).

The goal of the current study was to examine global functional network connectivity and organization in developmental dyslexia using the electroencephalogram (EEG) in resting-state data. Previous fMRI studies on resting-state data revealed relations between resting-state functional connectivity across the reading network with reading abilities in children and adults (Koyama et al., 2011, 2013; Schurz et al., 2014; Zhang et al., 2014). Other studies linked the strength of resting-state connectivity between the visual word recognition areas and the dorsal attention network to age and reading skills (Vogel et al., 2012, 2014). The latter studies attest to the utility of resting-state data to characterize the functional reading network (Hampson et al., 2006; Koyama et al., 2010).

In the current study we used graph analysis, which allows for modeling the organization of resting-state whole-brain functional connectivity networks during development (Stam, 2014). A 'graph' refers to an abstract representation of a network, consisting of a set of nodes (vertices) and connections between them (edges). Various graph measures allow for characterizing graph topologies in terms of the efficiency of information transfer and an optimal balance between 'segregation' and 'integration' (see reviews in Bullmore and Sporns, 2009, 2012). Thus, a 'small-world' network topology, characterized by a high clustering (related to high local connectedness and robustness) and a short path length (related to high global efficiency) has been proposed as a plausible configuration of highly efficient brain networks (Bassett and Bullmore, 2006). This topology combines features from ordered or regular networks (high clustering) and random networks (short path length).

A recent development in graph theory refers to minimum spanning tree (MST) analysis (Stam et al., 2014). A tree is a loop-less sub-graph derived from a weighted connectivity matrix, with a fixed number of nodes and edges; in the MST, the presence of a link is not defined by a given threshold in the connectivity weights (see Section 2). The advantage of MST analysis over conventional graph procedures is that it minimizes bias when performing direct comparisons between groups and experimental conditions (Tewarie et al., 2015). There are two extreme tree topologies; path- and star-like configurations. Path-like configurations consist of nodes that are all linked to two other nodes with the exception of the nodes at either end of the path. Nodes with only one link in a tree are referred to as 'leaf' nodes (or leaves) and the number of those nodes in a tree is the leaf number. Thus a path has a leaf number of two. In contrast, star-like configurations consist of a central node connected to all other nodes with only one link. Thus, a star consisting of $N$ nodes has a leaf number of $N-1$. Many different tree topologies are in between the two extreme configurations and they can be characterized using a variety of metrics (review in Van Mieghem, 2014). We will apply the tree measures that have been applied previously in EEG studies (see Section 2 below).

The MST analysis has been successfully applied to EEG data from different populations. A relatively early study indicated that patients with left vs. right temporal epilepsy could be reliably discriminated in terms of large scale functional networks emerging just prior to the onset of seizures (Lee et al., 2006). More recently, Fraschini et al., 2014 examined the effects of vagal nerve stimulation in patients with pharmaco-resistant epilepsy. MST analysis yielded a clear differentiation between responders vs. non-responders. Vagal nerve stimulation shifted the network towards a more star-like network architecture in responders but not in non-responders. Van Diessen et al. (2014) examined the effect of sleep deprivation on EEG networks in children diagnosed with focal epilepsy. MST analysis revealed a shift to a more path-like topology after sleep deprivation in children with focal epilepsy whereas a shift towards a more star-like configuration was observed in controls. Vourkas et al. (2014) performed a MST analysis on the EEG recorded in children with mathematical difficulties and typical controls during the performance of tasks with increasing difficulty. Although group differences were absent in this study the MST parameters suggested a more centralized and integrated network layout in the alpha bands of the EEG with increasing task demands. Most relevant to the present study, Boersma et al. (2013) applied MST analysis to resting-state EEG data of a large sample of 5- and 7-years old children. Developmental change was observed for the EEG alpha band. More specifically, the MST analysis yielded increases in diameter and eccentricity with advancing age while leaf number, degree and hierarchy decreased. This pattern of results was interpreted to suggest a more integrated network configuration in the 7- compared to the 5-years olds.

Collectively, the MST studies suggest this approach may provide a sensitive tool to assess condition or group differences in network configuration. Previously, graph analysis of magnetoencephalographic (MEG) data in dyslexic children and controls showed task-dependent dysfunctional long- and short-range functional connectivity in the dyslexic children (Vourkas et al., 2011). Another graph analysis from the same group of MEG data obtained during rest revealed less organized network configuration in dyslexic children (Dimitriadis et al., 2013). The current study will extend these findings by focusing on resting state EEG data and by performing a MST analysis on these data. The use of resting state data should indicate functional network differences between the groups that are not related to task-related strategies and that are indicative of the underlying architecture of oscillatory EEG activity. MST analysis goes beyond more conventional network analysis as (i) it allows an unbiased network representation; (ii) it provides a comparison between groups/conditions that is normalized; and (iii) it integrates features of small-worldness (clustering/path length) and scale-freeness (hubs) (e.g., Tewarie et al., 2015).

## 2. Methods

### 2.1. Participants

Twenty-nine third-grade dyslexic children (Mean age = 8.46; SD = 0.40) were recruited from a nation-wide center for dyslexia

**Table 1**
Sample characteristics and descriptive statistics showing reading accuracy and fluency scores.

| | Controls *M* (*SD*) | Dyslexics *M* (*SD*) | *p*-value | $\eta^2$ |
|---|---|---|---|---|
| *N* | 15 | 29 | | |
| Sex ratio (m:f) | 6:09 | 16:13 | | |
| Handedness (L:R)[*] | 2:10 | 2:27 | | |
| Age | 8.75 (0.31) | 8.96 (0.40) | 0.088 | 0.07 |
| RAVEN – IQ test[a] | 6.70 (1.51) | 7.11 (1.51) | 0.395 | 0.02 |
| 3DM word reading – *accuracy*[b] | | | | |
| High frequency | 99.28 (1.05) | 93.10 (5.93) | 0.000 | 0.27 |
| Low frequency | 98.32 (2.54) | 86.31 (14.48) | 0.003 | 0.19 |
| Pseudo | 88.70 (8.48) | 73.33 (17.43) | 0.003 | 0.20 |
| Total [T][c] | 51.40 (8.00) | 33.72 (12.58) | 0.000 | 0.37 |
| 3DM word reading – *fluency* [*T*] | | | | |
| High frequency | 54.27 (7.58) | 31.38 (6.14) | 0.000 | 0.74 |
| Low frequency | 56.80 (8.98) | 32.07 (6.46) | 0.000 | 0.72 |
| Pseudo | 54.93 (9.71) | 30.93 (6.37) | 0.000 | 0.70 |
| Total | 55.93 (9.51) | 31.00 (5.40) | 0.000 | 0.75 |
| One-minute test – *fluency* [SS][d] | 12.07 (2.94) | 3.97 (1.97) | 0.000 | 0.74 |
| Text reading – *fluency* [*T*][**] | 55.27 (8.41) | 33.21 (6.30) | 0.000 | 0.70 |
| 3DM spelling – accuracy [*T*] | 51.73 (8.62) | 36.21 (6.70) | 0.000 | 0.51 |
| 3DM spelling – fluency [*T*] | 54.33 (9.90) | 36.55 (6.01) | 0.000 | 0.57 |
| 3DM phoneme deletion – *accuracy* [*T*][**] | 53.73 (8.39) | 39.61 (8.32) | 0.000 | 0.41 |
| Letter-speech sound associations [*T*] | | | | |
| L-SS identification – *accuracy* | 46.87 (8.65) | 43.34 (12.99) | 0.350 | 0.02 |
| L-SS discrimination – *accuracy*[**] | 50.80 (10.28) | 44.43 (9.63) | 0.050 | 0.09 |
| L-SS identification – *fluency* | 51.53 (7.67) | 41.79 (6.97) | 0.000 | 0.30 |
| L-SS discrimination – *fluency*[**] | 51.73 (7.36) | 45.46 (8.95) | 0.025 | 0.12 |
| 3DM naming speed scores [*T*][**] | | | | |
| Letters | 50.93 (6.95) | 36.57 (8.05) | 0.000 | 0.45 |
| Numbers | 52.73 (10.67) | 36.21 (8.50) | 0.000 | 0.43 |
| Total | 50.80 (7.73) | 35.54 (9.15) | 0.000 | 0.42 |

[a] C scores ($M = 5$, SD = 2).
[b] Raw scores.
[c] *T* scores ($M = 50$, SD = 10).
[d] SS scores ($M = 10$, SD = 3).
[*] Data missing for 3 participants; typical $N = 12$.
[**] Data missing for one participant; dyslexics $N = 28$.

in the Netherlands.[1] All dyslexic children had a percentile score of 10 or lower on a standard reading test and they participated in the EEG recordings before starting their treatment program at the center. A group of 15 third-grade, control children (8.75 ± 0.31 years old) was recruited from several primary schools attended by children with the same socio-demographical background as the dyslexic group (see Table 1 for group characteristics). They had no history of reading difficulties and had a percentile score of 25 or higher on standard reading tests (see below). All participants were native Dutch speakers, received two and a half years of formal reading instruction in primary education. Children with below average IQ (IQ < 85 on a non-verbal IQ-test), uncorrected sight problems, hearing loss, diagnosis of ADHD or other neurological or cognitive impairments were excluded. The study was approved by the Ethical Review Board of the University and all parents or caretakers signed informed consent before the children participated.

[1] The current participants are part of a larger sample of 62 children taking part in the EEG recordings. From the original data set, resting-state data was not available for 3 participants due to complications during recording. Moreover, data from 6 participants were excluded due to excessive artifacts. In the remaining data ($N = 53$), the inspection of individual peak frequencies in the average spectra indicated that for the majority of participants the peak frequency fell within the low alpha (8–10 Hz) and high alpha (10–13 Hz) range (see Section 2.5). We discarded data from children with a peak frequency equal or lower than 8 Hz as this might bias subsequent analysis in the lower frequency bands. A total of 9 subjects were excluded; 5 dyslexics ($N = 29$) and 4 controls ($N = 15$). Demographic characteristics and reading scores of the complete sample are included in Supplementary Appendix A.

### 2.2. Behavioral measurements

A series of tests was used to assess the reading skills of the participants (Fraga González et al., 2015). The children took the tests at their school.

Word reading skills were measured using a Dutch version of the *One-minute test* (*Een-Minuut-Test*, EMT; Van den Bos et al., 1999), a time-limited test consisting of a list of 116 unrelated words of increasing difficulty. The number of correctly read words within 1 min serves as reading fluency score. Text reading fluency was assessed also using a test consisting of a coherent text of increasing difficulty. The children were asked to read the story out loud within 1 min (*Schoolvaardigheidstoets Technisch Lezen*; de Vos, 2007). In addition, the 3DM battery of tests (test reliability information available in *Dyslexia differential diagnosis*; 3DM, Blomert and Vaessen, 2009) was individually administered. The scores of the following 3DM subtests were used. *Word reading task*: contains visually presented high-frequency words, low-frequency words and pseudowords. Accuracy (% correct) and fluency (correct words in 1 min) were measured. *Rapid automatized naming (RAN)*: blocks of letters or numbers are presented and items have to be read as fast and accurately as possible. Fluency is the time in seconds needed to name a screen of 15 items. *Letter-speech sound (LSS) association tasks*: consist of identification and discrimination tasks. In the identification task an aurally presented speech sound has to be matched to one out of four visually presented letters. In the discrimination task the child has to judge whether the speech sound and letter on the screen are congruent or incongruent. *Computerized spelling:* words are aurally presented and visually displayed

on screen with missing letters. Participants have to select the missing letter out of four alternatives. For the last two subtests, accuracy (% correct) as well as response time (sec/item) is measured.

Finally, the *RAVEN Coloured Progressive Matrices* was used to obtain an estimate of fluid IQ (RAVEN CPM; Raven et al., 1998) and the Child Behavior Checklist (CBCL) was completed by the parents to exclude any additional behavioral problems (Achenbach et al., 2008).

### 2.3. Procedure and equipment

EEG recordings were taken within a period of around 4 months and took place in a video-controlled, dimly lit and air conditioned laboratory room. The participant and a lab assistant were together at all times in the room while the experimenter controlling the recording was in an adjacent room. The 2 min eyes-closed resting-state baseline was recorded at the beginning of a longer experimental session (around 2 h long, including visual and audio-visual tasks). Children were instructed to keep their eyes closed and, when ready, to make a button press to initiate the eyes-closed resting state EEG recording. Participants were monitored at all times to ensure they complied to the instructions during the baseline recording and that children did not show behavioral indications of drowsiness or sleep onset during the recording.

### 2.4. EEG recording and signal processing

The EEG data were collected using a 64 channels Biosemi ActiveTwo system (Biosemi, Amsterdam, Netherlands). EEG was recorded DC (low-pass: 5th order sync digital filter) with a 1024 Hz sample rate. The Biosemi system uses two additional electrodes (Common Mode Sense [CMS] and Driven Right Leg [DRL]) creating a feedback loop to replace the conventional ground electrode (see www.biosemi.com/faq/cms&drl.htm for details). The CMS electrode served as online reference. The 64 electrodes were distributed on the scalp according to the 10–20 International system and applied using an elastic electrode cap (Electro-cap International Inc.). Six external Flat-Type Active electrodes were used; four electrodes for recording the vertical and horizontal electro-oculogram (EOG) and two electrodes were placed at mastoids for off-line reference.

Continuous EEG data were imported in EEGLAB v.11.0.0.0b (Delorme and Makeig, 2004), an open source toolbox for Matlab (Mathworks, Inc.), using the averaged mastoids as initial off-line reference. A two minutes long epoch was selected, time-locked to the button press indicating the start of the eyes-closed resting-state recording.

The 2 min EEG epoch was imported in Brain Vision Analyzer (Version 2.0.1.5528, ©Brain Products) for further preprocessing. After importing, spline interpolation was applied to channels with excessive artifacts. In the control group, interpolation was applied to data from 10 subjects (a maximum of 5 electrodes in one subject); in the dyslexic group interpolation was applied to data from 8 subjects (a maximum of 5 electrodes in one subject). Data were segmented in 30 epochs of 4 s (4096 sample points per epoch). The epochs were visually inspected for eye blinks or muscle artifacts. For each subject 10 artifact-free epochs were selected and exported to ASCII files.

The artifact-free epochs of 4 s were imported in Brainwave v0.9.117 (developed by C.S.; freely available at http://home.kpn.nl/stam7883/brainwave.html) where data were re-referenced to the average of all scalp channels before performing spectral power analysis, functional connectivity and MST metrics.

For the analysis of connectivity strength (measured with phase lag index; see Section 2.6), besides mean connectivity, the following sub-averages were calculated: frontal (including the electrodes Fp1, Fp2, AF3, AF4, AF7, AF8, F1, F2, F3, F4, F5, F6, F7 and F8); central (including the electrodes FC1, FC2, FC3, FC4, FC5, FC6, C1, C2, C3, C4, C5, C6, CP1, CP2, CP3, CP4, CP5 and CP6); temporal (including the electrodes FT7, FT8, T7, T8, TP7 and TP8) and parietal-occipital (including the electrodes O1, O2, PO3, PO4, PO7, PO8, P1, P2, P3, P4, P5, P6, P7, P8, P9 and P10). The mean connectivity between the electrodes included in each sub-average was calculated. These sub-averages were chosen to examine strength of both short-range and long-range connectivity across broad cortical regions that previous studies have found relevant to reading and dyslexia. Note that the graph measures, which are the main focus of the present analysis, were derived from the complete connectivity matrix including the 64 scalp electrodes.

### 2.5. Spectral power

Spectral power was calculated for all EEG channels using Fast Fourier Transformation (FFT) in Brainwave, with a frequency resolution of 1/4 s = 0.25 Hz. The relative power values were calculated for the following frequency bands: delta (0.5–4 Hz), theta (4–8 Hz), alpha (8–13 Hz), beta (13–30 Hz) and gamma (30–48 Hz). The broad alpha range was used instead of the lower alpha (8–10 Hz) and upper alpha (10–13 Hz) as some participants showed an average peak frequency within the upper alpha range. Power values were averaged over epochs.

### 2.6. Functional connectivity

The phase lag index (PLI) was used to calculate functional connectivity between all 64 electrodes for each frequency band and in each segment, separately. The PLI measures phase synchronization based on the asymmetry of the distribution of instantaneous phase differences between two signals, which is determined using the analytical signal based on the Hilbert transformation (Stam et al., 2007). The PLI is less sensitive to common sources since the zero-lag synchronization is removed from the analysis (Porz et al., 2014). Furthermore, the PLI quantifies the relative phase distribution's asymmetry; that is, that the likelihood that the phase difference $\Delta\varphi$ will be in the interval $-\pi < \Delta\varphi < 0$ is different from the likelihood that it will be in the interval $0 < \Delta\varphi < \pi$. This implies the presence of a consistent, nonzero phase difference ('lag') between two time series. The distribution is expected to be symmetric if there is no coupling or if the median phase difference is equal to or centers around a value of 0 mod $\pi$. The PLI is obtained from time series of phase differences $\Delta\varphi(t_k)$, $k = 1 \ldots N$ by means of:

$$\mathrm{PLI} = |<\mathrm{sign}[\sin(\Delta\varphi(t_k))]>|$$

Here sign is the signum function. The PLI ranges between 0 and 1. A PLI of zero indicates either no coupling or coupling with a phase difference centered around 0 (mod $\pi$). A PLI of 1 indicates perfect phase locking at a value of $\Delta\varphi$ different from 0 (mod $\pi$). The stronger this nonzero phase locking is, the larger PLI will be.

### 2.7. Minimum spanning tree

The minimum spanning tree (MST) sub-graph was calculated for each PLI matrix derived per segment. A schematic of the analytic steps is shown in Fig. 1. The MST is a unique sub-graph based on a weighted matrix that connects all nodes of the network but does not contain circles or loops. The MST always contains $m = N - 1$ links, where $N$ is the number of nodes. The MST was constructed by applying Kruskal's algorithm (Kruskal, 1956). This algorithm orders the distance of all links in an ascending order followed by the construction of the MST with the link of the shortest distance, and then adding the following shortest distance link until all nodes are connected in a loop-less sub-graph. If adding a

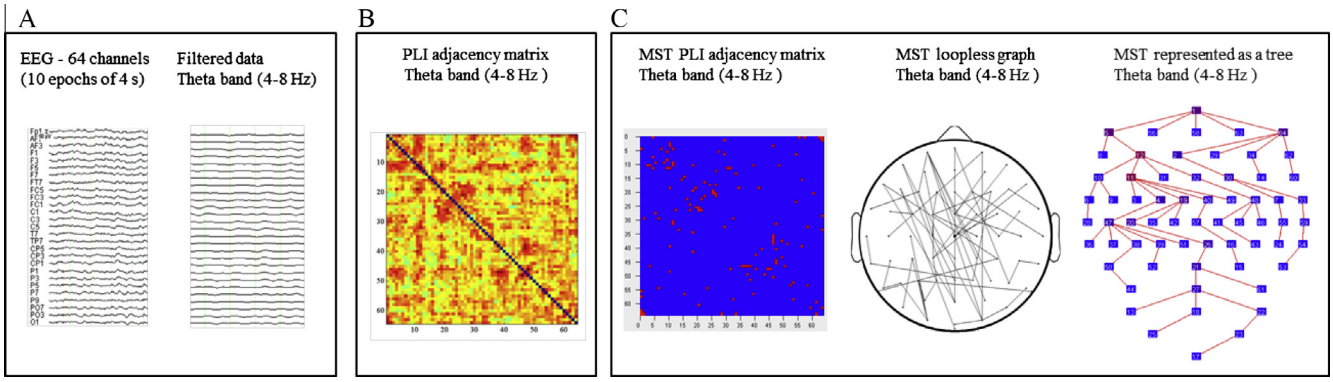


**Fig. 1.** Schematic of the graph analysis. First, artifact-free epochs are filtered for each frequency band (A). Secondly, the functional connectivity matrix based on Phase lag index (PLI) is calculated for each frequency band and epoch (B). Finally, the Kruskal's algorithm is applied to obtain the minimum spanning tree (MST) matrix (C-left); the resulting loopless graph is displayed on a scalp projection (C-middle) and as a tree (C-right). The tree view shows the hierarchical structure of the graph starting from an arbitrary root node (in this case FP1), the color map of the nodes from blue to red represents lower to higher betweenness centrality. For illustrative purposes this figure shows the MST obtained from the PLI matrix averaged across epochs and subjects of the control group ($N = 15$).

**Table 2**
MST measures summary.

| | | |
|---|---|---|
| $N$ | Nodes | Number of nodes in MST |
| $m$ | Links | Number of links in the MST |
| | Degree | Number of neighbors for a given node in the MST |
| $L$ | Leaf fraction | Fraction of nodes with degree = 1 (leafs) in the MST |
| $d$ | Diameter | Largest distance between any two nodes of the tree |
| | Eccentricity | Longest distance between a reference node and any other node |
| $BC$ | Betweenness centrality | Fraction of all shortest paths that pass through a particular node |
| $k$ | Kappa | Measure of the broadness of the degree distribution (degree divergence) |
| $Th$ | Tree hierarchy | A hierarchical metric that quantifies the trade-off between large scale integration in the MST and the overload of central nodes |
| $R$ | Degree correlation | Correlation between the degrees of a node and the degree of the neighboring vertices to which it is connected |

new link results in the formation of a cycle, this link is skipped. In the current case, we use a maximum spanning tree, which is equivalent to an MST based upon 1-PLI, which represents the subnetwork with maximum connectivity.

MST metrics provides information about the topological properties of the tree. The following tree measures were used in this study: Degree, leaf number, betweenness centrality (BC), eccentricity, diameter, hierarchy ($T_h$), and degree correlation ($R$). The measures are summarized in Table 2 and examples of tree topologies with increasing leaf number are presented in Fig. 2 (a detailed description in Stam et al., 2014). The degree of a node is its number of connections (edges), and the leaf fraction ($L$) represents the number of nodes on the tree with degree = 1. The leaf number has a lower bound of 2 and upper bound of $N - 1$. The leaf number presents an upper bound to the diameter of the MST, which is the largest distance between any two nodes of the tree. The upper limit of the diameter is $d = m - L + 2$, which implies that the largest possible diameter will decrease with the increasing leaf number. Eccentricity of a node is defined as the longest distance between that node and any other node and is low if this node is central in the tree. The BC of a node $u$ is the number of shortest paths between any pair of nodes $i$ and $j$ that are running through $u$, divided by the total number of paths between $i$ and $j$. The BC value ranges between 0 and 1 since it is a fraction. The BC relates to the importance of a node within the network. The nodes with the highest BC have the highest load. For instance, in a star-like tree, the central node has a BC of 1 and it could be easily overloaded, while

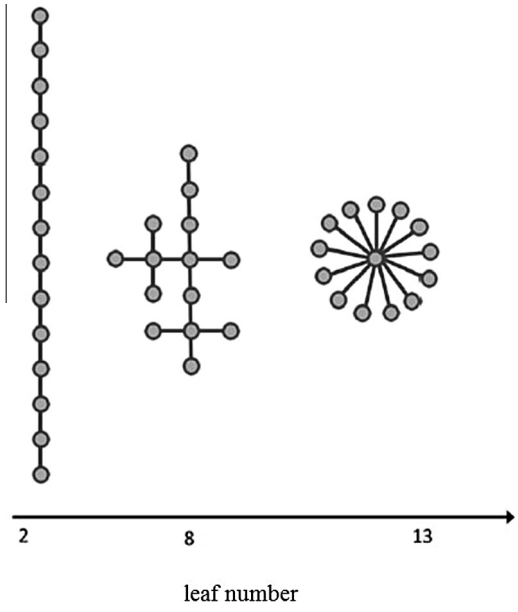


**Fig. 2.** Examples of trees for increasing leaf number including the two extreme forms of trees. All of them have 14 nodes (circles) and 13 edges (lines). On the left a line-like tree with the lowest possible leaf number which is 2. The middle example shows a tree configuration with eight leaf nodes. On the right, a star-like tree with the highest possible leaf number which equals the number of edges.

the leaf nodes have a BC of 0. Degree, eccentricity and BC are different measures for relative nodal importance and may indicate the critical nodes in a tree.

For a tree topology to result in optimal network performance, it should conform to two criteria. Firstly, efficient communication would require a small diameter. Secondly, the tree topology would require preventing overload of hub nodes by setting a maximal $BC_{max}$ for any tree node. The balance between these two criteria is reflected by the tree hierarchy ($T_h$) measure (Boersma et al., 2013), which is defined as:

$$T_H = \frac{L}{2m\mathrm{BC}_{\max}} \tag{1}$$

To assure $T_h$ ranges between 0 and 1, the denominator is multiplied by 2. If $L = 2$ (line-like topology), and $m$ approaches infinity, then $T_h$ approaches 0. If $L = m$ (star-like topography), then $T_h$ approaches 0.5. For leaf numbers in between these extreme values, $T_h$ has higher values.

Finally, the degree correlation is an index of whether the degree of a node is correlated with the degree of its neighboring vertices to which it is connected. A positive degree correlation indicates that the graph is assortative; if the degree correlation is negative the graph is called disassortative. The degree correlations can be quantified by computing the Pearson correlation coefficient of the degrees of pairs of nodes connected by an edge. Interestingly, most social networks tend to be assortative, while most technological and biological networks tend to be disassortative (Newman, 2003).

### 2.8. Statistical analysis

One-way ANOVAs were used for group comparisons in behavioral measures, relative power, PLI averages and MST measures. As indicated above, PLI and MST were calculated per segment and then averaged for each participant. Prior to analysis, the PLI and MST measures were transformed to their natural logarithm, $y = \ln(x)$, to obtain normal distributions. For the behavioral analyses, standardized scores were used instead of raw scores, in order to assess the child's position within the distribution of a normative sample. Due to reduced variance, no reliable norm scores were available for the accuracy measures of the three subtasks of the 3DM word reading; thus raw scores were used for these measures. Additionally, for the MST measures, Bonferroni correction for multiple comparisons was applied to $p$ values for each frequency band. Finally, to examine the relation between tree-derived measures and reading, regression analysis was performed in dyslexics and controls separately for the MST measures in which we found group differences and the main reading scores.

The same set of analyses was performed on the data of a subsample of 15 randomly selected dyslexics to evaluate whether different sample sizes dyslexic children ($n = 29$) and controls ($n = 15$) had any effect in the group differences. The main pattern of results reported below did not change and it is presented in Supplementary Appendix B.

## 3. Results

### 3.1. Behavior

The results of the ANOVAs for reading accuracy and speed measures are shown in Table 1. The table shows a deficit in dyslexics that is mainly manifested by substantial differences in the reading fluency measures. The dyslexic group attained reasonably high levels of accuracy, although significantly lower than those of the control group. With regard to the letter-speech sound measures, only the fluency scores were sensitive to group differences.

### 3.2. Spectral power and functional connectivity

The power spectra averaged across all electrodes for each group are shown in Fig. 3. Controls and dyslexics both showed prominent peak frequencies in the alpha band, which did not differ between groups. The ANOVAs performed on the relative power values in each frequency band revealed no significant differences (in the total average or regional sub-averages) between groups. For each frequency band outliers and extreme values in relative power were detected and excluded for the subsequent analyses of connectivity and graph measures. Outliers and extreme values were defined based on 1.5 inter-quartile range steps. Accordingly, for the theta band 2 subjects from the dyslexic group were excluded ($N = 27$). For the alpha band 1 subject from the dyslexic group was excluded ($N = 28$). No outliers or extreme values were detected in the delta, beta or gamma band.

The PLI total values and sub-averages were calculated for each frequency band. The ANOVAs yielded no significant differences in functional connectivity (total network or sub-networks) between groups (all $p$'s > .05). The total PLI values for each frequency band are presented in Tables 3 and 4.

### 3.3. MST analysis

MST analysis yielded significant between group effects in the theta band (see Table 3 and Fig. 4). Leaf fraction, reflecting the integration of information within the network, was significantly lower in dyslexics relative to typical readers, $F$ (1, 40) = 10.24, $p = .003$, $\eta^2 = 0.20$. The group effect on diameter, representing the efficiency of communication between the nodes, was significant also, $F$ (1, 40) = 4.27, $p = .045$, $\eta^2 = 0.10$, indicating higher diameter in dyslexics relative to controls. The group effect on eccentricity, relating to node centrality, just fell short of significance, $F$ (1, 40) = 3.47, $p = .070$, $\eta^2 = 0.08$, suggesting a trend for higher eccentricity in dyslexics compared to controls. These group differences are displayed in Fig. 5. Collectively these results indicate a less integrated network organization in dyslexic children compared to controls.

For the alpha band, the group effects on diameter and eccentricity just failed to reach significance, $p = .080$ and $p = .098$, respectively, suggesting trends for higher diameter and eccentricity in dyslexics relative to controls.[2] Finally, for the gamma band, the ANOVA revealed a somewhat higher hierarchy in controls relative to the dyslexic children but this effect just failed to reach significance, $F$ (1, 40) = 3.89, $p = .055$, $\eta^2 = 0.09$. Group effects in all other measures and frequency bands were not significant, $ps > .124$. Moreover, there were no significant correlations between MST measures and reading performance.

## 4. Discussion

The present study examined the topological characteristics of brain networks in dyslexics and controls by applying MST analysis to eyes-closed resting state EEG. The present results suggest that compared to controls, dyslexics may present differences in the way spontaneous oscillatory activity is organized. Our results showed a clear dissociation between PLI connectivity analyses vs. MST analyses of global network organization. That is, the PLI analyses failed to reveal differences in connectivity strength between groups whereas the MST analyses yielded between groups differences in network organization as revealed in the theta band. The MST method should correct for potential bias in comparing networks (Stam et al., 2014). Our pattern of findings presents another illustration of the differences between connectivity vs. network analysis of EEG data (see also Stam and van Straaten, 2012). More specifically, the MST analysis showed for dyslexic children a smaller leaf fraction indicating less network integration compared to controls. In addition, there was a significant group difference for diameter suggesting less communication between nodes of the network in dyslexics compared to controls. In terms of the extreme tree topologies, the current pattern of results suggests a more

[2] In a control analysis including peak frequency as a covariate the main results in the theta band for leaf number remained significant ($F = 9.94$, $p = .003$, $\eta^2 = 0.20$), while for the metric of diameter the group difference just fell short of significance ($F = 4.07$, $p = .051$, $\eta^2 = 0.09$). Moreover, we performed additional analysis in the separate alpha 1 (8–10 Hz) and alpha 2 (10–13 Hz) frequency bands, similarly to other studies (e.g. Tewarie et al., 2014, Van Diessen et al., 2014). The group comparison in the alpha1 band revealed a significant effect in leaf number ($F = 5.57$, $p = .023$, $\eta^2 = 0.12$), indicating a lower leaf number in dyslexics relative to control readers. No significant group effects were found in the other metrics. In the alpha 2 band, we did not find significant group differences for any of the MST metrics analyzed.

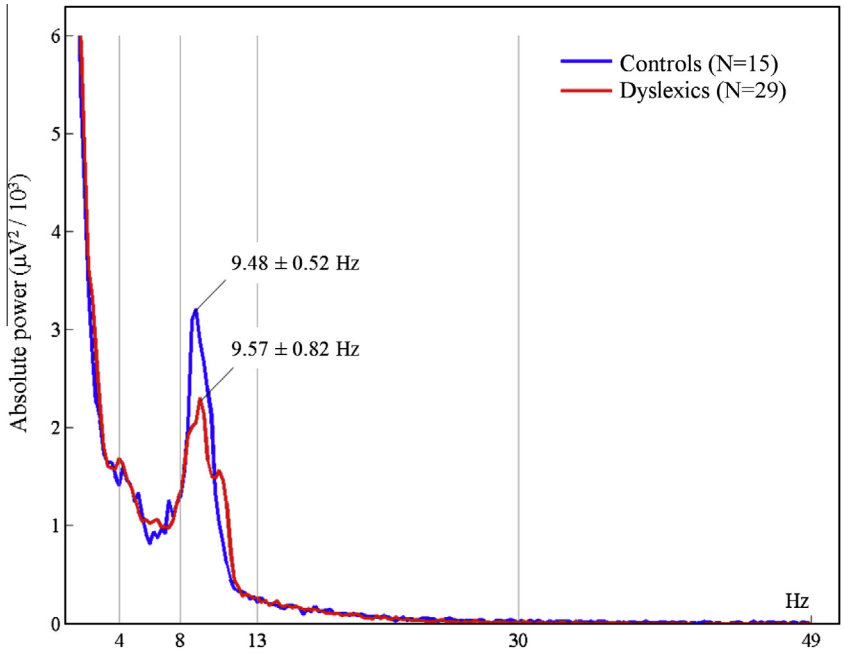


**Fig. 3.** Power spectra averaged across 64 EEG scalp channels for the control and the dyslexic group.

**Table 3**
PLI average and MST measures.

| | | Typical ($N$ = 15) | | Dyslexics ($N$ = 29) | | $F$ | $p$ value | $\eta^2$ |
|---|---|---|---|---|---|---|---|---|
| | | $M$ | ($SD$) | $M$ | ($SD$) | | | |
| Delta | PLI | 0.202 | (0.012) | 0.207 | (0.013) | 1.94 | 0.171 | 0.04 |
| | Degree | 0.163 | (0.022) | 0.16 | (0.022) | 0.31 | 0.580 | 0.01 |
| | Leaf | 0.583 | (0.012) | 0.576 | (0.020) | 1.37 | 0.248 | 0.03 |
| | Eccentricity | 0.168 | (0.010) | 0.170 | (0.011) | 0.36 | 0.552 | 0.01 |
| | Kappa | 3.551 | (0.259) | 3.501 | (0.270) | 0.37 | 0.543 | 0.01 |
| | Diameter | 0.216 | (0.013) | 0.219 | (0.014) | 0.33 | 0.568 | 0.01 |
| | BC | 0.704 | (0.026) | 0.698 | (0.033) | 0.32 | 0.577 | 0.01 |
| | Degree correlation | −0.325 | (0.030) | −0.321 | (0.039) | 0.22 | 0.643 | 0.00 |
| | Hierarchy | 0.418 | (0.015) | 0.417 | (0.023) | 0.03 | 0.865 | 0.00 |
| Theta[a] | PLI | 0.176 | (0.008) | 0.174 | (0.009) | 0.70 | 0.408 | 0.02 |
| | Degree | 0.152 | (0.011) | 0.148 | (0.015) | 0.86 | 0.359 | 0.02 |
| | Leaf | **0.584** | (**0.013**) | **0.569** | (**0.015**) | **10.31** | **0.003**[*] | **0.20** |
| | Eccentricity | *0.169* | (*0.011*) | *0.174* | (*0.008*) | *3.47* | *0.070* | *0.08* |
| | Kappa | 3.415 | (0.149) | 3.341 | (0.165) | 2.14 | 0.151 | 0.05 |
| | Diameter | **0.216** | (**0.015**) | **0.224** | (**0.011**) | **4.27** | **0.045** | **0.10** |
| | BC | 0.701 | (0.022) | 0.696 | (0.023) | 0.49 | 0.489 | 0.01 |
| | Degree Correlation | −0.327 | (0.037) | −0.319 | (0.031) | 0.55 | 0.463 | 0.01 |
| | Hierarchy | 0.419 | (0.015) | 0.412 | (0.016) | 2.13 | 0.152 | 0.05 |
| Alpha[b] | PLI | 0.209 | (0.033) | 0.200 | (0.037) | 0.68 | 0.413 | 0.02 |
| | Degree | 0.187 | (0.028) | 0.185 | (0.033) | 0.11 | 0.744 | 0.00 |
| | Leaf | 0.623 | (0.030) | 0.609 | (0.027) | 2.59 | 0.115 | 0.06 |
| | Eccentricity | *0.154* | (*0.013*) | *0.160* | (*0.011*) | *2.86* | *0.098* | *0.07* |
| | Kappa | 3.967 | (0.398) | 3.892 | (0.466) | 0.37 | 0.545 | 0.01 |
| | Diameter | *0.197* | (*0.018*) | *0.206* | (*0.015*) | *3.22* | *0.080* | *0.07* |
| | BC | 0.713 | (0.025) | 0.712 | (0.032) | 0.03 | 0.862 | 0.00 |
| | Degree Correlation | −0.345 | (0.028) | −0.352 | (0.038) | 0.29 | 0.593 | 0.01 |
| | Hierarchy | 0.441 | (0.018) | 0.432 | (0.024) | 1.74 | 0.194 | 0.04 |

*Notes*: bold text represents significant results ($p < 0.05$); italic text represents results at trend level. MST, minimum spanning tree; PLI, phase lag index; BC, betweenness centrality.

[*] Significant after Bonferroni correction at $p = 0.059$ (i.e., $p < 0.006$).

[a] Two outliers based on spectral power excluded; Dyslexics $N = 27$.

[b] One outlier based on spectral power excluded; Dyslexics $N = 28$.

path-like configuration in dyslexic children and a more star-like topology in typically reading children (see Fig. 4).

The current group difference in network topology is indicative of a less integrated network configuration in dyslexic children compared to controls (Olde Dubbelink et al., 2014; Stam et al., 2014). This finding is in accordance with previous functional connectivity studies suggesting a disrupted network structure and mixed patterns of connectivity abnormalities in dyslexia (Frye et al., 2012; Koyama et al., 2013). A relevant consideration when interpreting the current results is the relation between

**Table 4**
PLI average and MST measures.

| | | Typical ($N = 15$) | | Dyslexics ($N = 29$) | | $F$ | $p$ value | $\eta^2$ |
|---|---|---|---|---|---|---|---|---|
| | | $M$ | ($SD$) | $M$ | ($SD$) | | | |
| Beta | PLI | 0.099 | (0.006) | 0.101 | (0.010) | 0.43 | 0.514 | 0.01 |
| | Degree | 0.160 | (0.019) | 0.162 | (0.019) | 0.09 | 0.770 | 0.00 |
| | Leaf | 0.582 | (0.018) | 0.580 | (0.022) | 0.07 | 0.796 | 0.00 |
| | Eccentricity | 0.168 | (0.010) | 0.168 | (0.009) | 0.00 | 0.958 | 0.00 |
| | Kappa | 3.516 | (0.244) | 3.542 | (0.275) | 0.08 | 0.773 | 0.00 |
| | Diameter | 0.216 | (0.013) | 0.216 | (0.012) | 0.06 | 0.811 | 0.00 |
| | BC | 0.691 | (0.026) | 0.702 | (0.021) | 2.28 | 0.138 | 0.05 |
| | Degree correlation | −0.319 | (0.027) | −0.316 | (0.040) | 0.18 | 0.675 | 0.00 |
| | Hierarchy | 0.425 | (0.015) | 0.417 | (0.020) | 1.72 | 0.197 | 0.04 |
| Gamma | PLI | 0.092 | (0.006) | 0.091 | (0.006) | 0.04 | 0.840 | 0.00 |
| | Degree | 0.224 | (0.041) | 0.214 | (0.061) | 0.69 | 0.410 | 0.02 |
| | Leaf | 0.637 | (0.034) | 0.621 | (0.038) | 2.04 | 0.160 | 0.05 |
| | Eccentricity | 0.152 | (0.011) | 0.158 | (0.015) | 2.02 | 0.162 | 0.05 |
| | Kappa | 4.587 | (0.875) | 4.468 | (1.381) | 0.41 | 0.528 | 0.01 |
| | Diameter | 0.196 | (0.014) | 0.205 | (0.019) | 2.31 | 0.136 | 0.05 |
| | BC | 0.725 | (0.027) | 0.725 | (0.032) | 0.00 | 0.942 | 0.00 |
| | Degree correlation | −0.366 | (0.031) | −0.356 | (0.040) | 0.89 | 0.350 | 0.02 |
| | *Hierarchy* | *0.443* | (*0.020*) | *0.431* | (*0.020*) | *3.89* | *0.055* | *0.09* |

*Notes:* italic text represents results at trend level; MST, minimum spanning tree; PLI, phase lag index; BC, betweenness centrality.

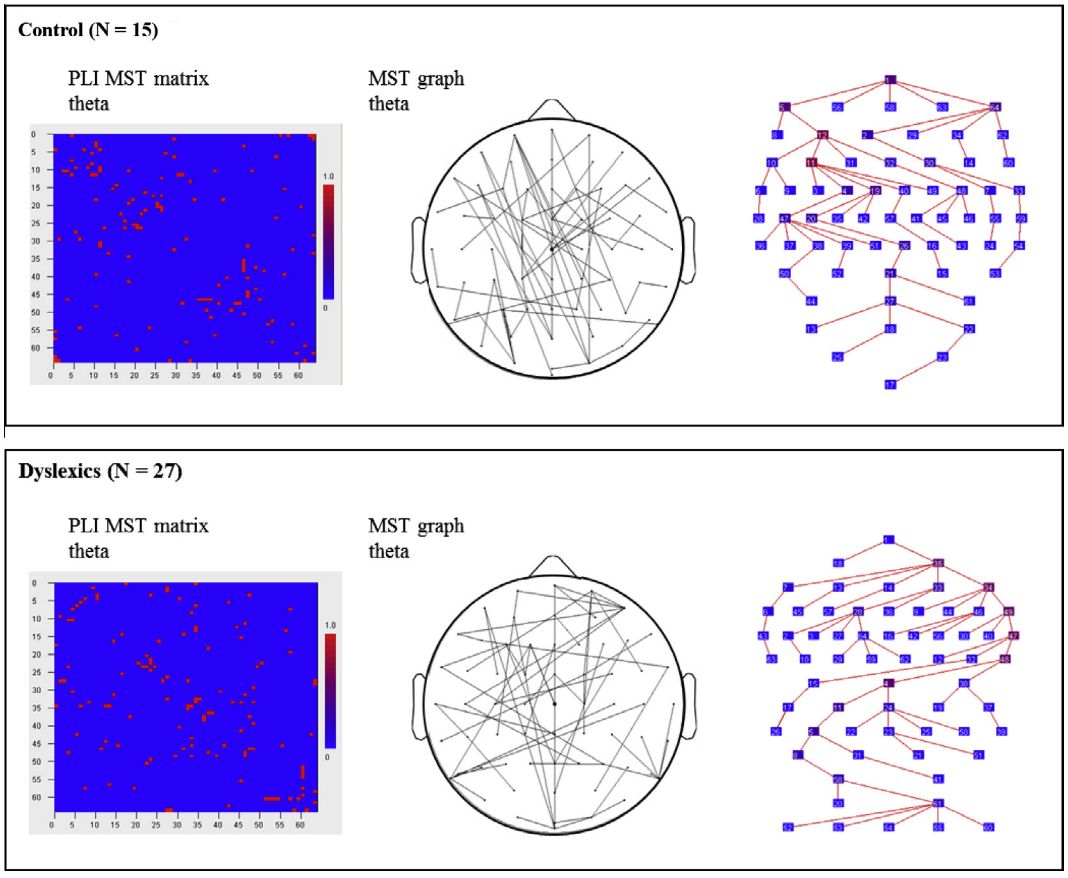


**Fig. 4.** MST matrices (left panels) and MST graph in scalp view (center panel) and tree view (right panel) for the theta band for controls (above) and dyslexics (below). For illustrative purposes the MST algorithm was performed on the averaged PLI matrices.

MST measures and more conventional graph metrics pertaining to network models such as small-world and scale-free networks. Tewarie et al. (2015) examined this relation by performing an extensive and systematic series of simulation studies. We observed for dyslexic children a lower leaf fraction and a trend for higher diameter relative to controls. Tewarie et al. (2015) observed that these two measures are strongly related to path length. MST leaf was negatively related to path length. More specifically, MST leaf was low for trees derived from regular networks and increased as these networks became more random. MST diameter, on the other hand, was positively related to path length. That is, diameter increased as networks became more regular. This finding is

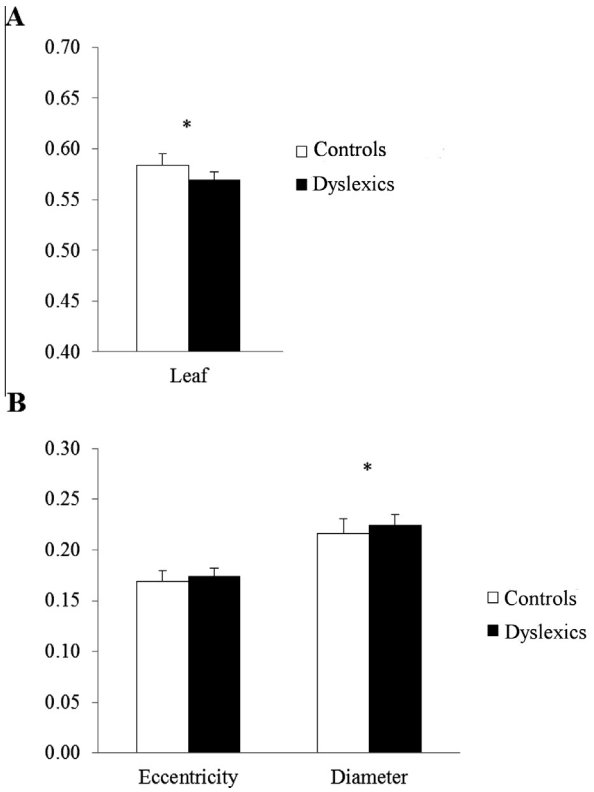


**Fig. 5.** (A) Group averages for leaf fraction, (B) eccentricity and diameter measures of the MST. Open bars refer to controls and filled bars to dyslexics. $^{*}p < 0.05$.

consistent with a recent study that examined the topology of structural networks in Chinese dyslexics in which a longer path length was observed for dyslexics relative to controls (Liu et al., 2015). Interestingly, in the Tewarie et al. (2015) simulation study, MST leaf fraction and diameter were also strongly related to the 'scale freeness' of the network. In particular, leaf fraction increased from regular to random networks and it was much larger for scale-free networks. Accordingly, the current results may also indicate a deviation from scale-free topologies that is larger in dyslexics compared to controls. A scale-free topology is indicative of the presence of highly connected hub nodes in the network (Stam, 2014). In this regard, the current findings may suggest dysfunctional hub nodes in dyslexia.

It should be emphasized that the main group differences in network organization were found in the theta band. The present results are consistent with previous research on functional and scaling aspects of oscillatory activity. Regarding general properties of the brain as an oscillatory system, research suggests that slow oscillations such as theta recruit large networks whereas higher frequencies are more confined to smaller networks (Buzsáki and Draguhn, 2004). Further, it is proposed that synchronous activity of lower frequency bands such as theta, mediate long range integration between processes involving several cortical areas (von Stein and Sarnthein, 2000). More specifically, theta frequencies have been related to long range interactions during top-down processes such as working memory retention (von Stein and Sarnthein, 2000). In relation language-specific functions, it has been suggested that synchronous theta activity may play an important role in speech processing (Luo and Poeppel, 2007; Poeppel et al., 2008) and language comprehension (Bastiaansen et al., 2008). Finally, the findings of current study support previous evidence suggesting abnormalities in theta oscillations associated with reading difficulties (Arns and Peters, 2007; Goswami, 2011; Klimesch, 1999; Marosi et al., 1995; Spironelli et al., 2008). Previous reports of theta band abnormalities in dyslexics or poor readers relative to controls include atypical lateralization in several reading tasks (Spironelli et al., 2008), increased power in frontal and temporal regions at rest (Arns and Peters, 2007), higher coherence (Marosi et al., 1995) and deficits in temporal sampling of phonological information (see review in Goswami, 2011). The current results extend previous findings linking abnormalities in the theta band to reading impaired groups by showing a less integrated network configuration in dyslexics' theta spontaneous oscillatory activity.

The current results showed also a between-group effect in the gamma band that just fell short of significance. The dyslexic children showed a lower tree hierarchy than controls. It should be noted, however, that the gamma band in scalp EEG recordings may be strongly affected by muscle artifact (Whitham et al., 2007). Consequently, a previous study using graph analysis excluded the higher frequency gamma band from analysis (Lee et al., 2010). In this regard, we hesitate to interpret the current findings for the gamma band, the more so because we are dealing with child data that are typically more affected by muscle artifact compared to adult participants.

It should be noted that the current study defined a broad alpha band (see Section 2.5). Previously, it has been suggested that lower and upper frequency alpha bands may be involved in different cognitive processes (see a review of some of these issues in van Diessen et al., 2015). In addition, individual peak frequency varies with age and state of wakefulness (Klimesch, 1999). Given the current scope and focus on resting-state and graph metrics, we opted for a broad alpha band definition to avoid biases from individual peak variability. Future studies could systematically investigate these issues and provide a more detailed description of the cognitive processes associated with the frequency bands in which network metrics are calculated.

The MST metrics of the EEG obtained during rest did not relate to the reading measures differentiating children with dyslexia from controls. Previously, Dimitriadis et al. (2013) did observe a positive relation between local efficiency of temporo-parietal networks in the beta band of the resting-state EEG and word reading measures in children with reading difficulties but not in typical controls. Similarly, Vourkas et al. (2011) reported significant correlations between graph metrics and phonological decoding ability but this relation was obtained for task-related EEG. In view of the limited studies available to date we are reluctant to interpret the current absence of a relation between reading ability measures and MST metrics. Future studies should examine the potential relations between these measures more systematically by comparing both resting-state and task-related EEG measures.

There are a few limitations to the current study. First, the current study used a modestly sized EEG montage (64 electrodes). Although MST metrics are not affected by connectivity strength and network density, some measures are sensitive to network size. Thus, our results should be replicated by using a high-density electrodes array, or preferably MEG source space networks, to assess relative nodal importance in network performance. Secondly, although PLI is more robust than other connectivity measures to methodological problems such as volume conduction (Stam et al., 2007), it is yet unclear how interpolation may affect connectivity measures. At some instances we had to resort to interpolation and the potential effects of interpolation should be examined more systematically. The current assessment of this issue suggests that, in view of the limited number of interpolations, it seems unlikely that interpolation impacted the connectivity weights. Moreover, a control analysis including only participants without interpolated data continued to show the between-groups effect on leaf number. The results of the control analysis are reported in Supplementary Appendix C. Further, in the current study, the PLI sub-averages dif-

fered in the number of electrodes and we cannot exclude the possibility that between-group differences in signal-to noise ratio might have affected our MST metrics. It should be noted, however, that the Tewarie et al. (2015) simulation studies indicated that the MST metrics are quite robust to noise. Finally, another potential limitation relates to the stability of our network measures. The current selection of segments was constrained by a relatively short baseline recording (2 min) and the presence of artifacts which are common in children EEG resting-state data. Because of this, we could not perform additional analyses on the effects of various epoch length in our graph and connectivity strength metrics. Importantly, however, these issues were systematically examined in a recent study suggesting that MST metrics derived from PLI are almost unaffected by epoch length and produce stable results also for short epochs (Fraschini et al., 2016). Those results suggest an advantage of tree-derived metrics when comparing results across studies in contrast with traditional graph metrics.

## 5. Conclusion

In conclusion, the global organization of functional brain networks may be compromised in dyslexics. The current MST analysis indicated a more path-like topology in dyslexics compared to controls for the EEG theta band. This finding suggests a less integrated network configuration in dyslexia. More specifically, the current results might indicate less efficient long-range connections in dyslexics, which would be in line with evidence suggesting disrupted connectivity between the distant cortical areas of the reading network (Sandak et al., 2004). The current findings also extend previous evidence suggesting abnormalities in connectivity across multiple brain networks beyond the reading network in dyslexics (Finn et al., 2014). The notion that dyslexics may present differences in widespread topology of brain connectivity would be compatible with evidence and theoretical approaches suggesting deficits in general sensory and attentional functions (e.g. visuospatial attention, visual attention span, auditory processing, etc.). Importantly, MST metrics could help characterizing the heterogeneity within dyslexia, as different underlying deficits may result in similar reading impairments. Future studies employing MST analysis might want to adopt a longitudinal perspective in examining the developmental trajectories of network organization during reading acquisition. Furthermore, it would be of considerable interest to examine how functional network organization is changed following reading intervention (e.g., Koyama et al., 2013).

## Acknowledgements

We dedicate this paper to our co-author professor Leo Blomert. His contributions to the initial stages of the project prior to his untimely death were significant. This project is part of the research program "Fluent reading neurocognitively decomposed: The case of dyslexia – HCMI 10-59" funded by the Netherlands Initiative Brain and Cognition, a part of the Organization for Scientific Research (NWO) under grant number 056-14-015. The funders had no role in study design, data collection and analysis, decision to publish, or preparation of this manuscript.

*Conflict of interest:* None of the authors have potential conflicts of interest to be disclosed.

## Appendix A. Supplementary data

Supplementary data associated with this article can be found, in the online version, at http://dx.doi.org/10.1016/j.clinph.2016.06.023.

## References

Achenbach TM, Becker A, Döpfner M, Heiervang E, Roessner V, Steinhausen HC, Rothenberger A. Multicultural assessment of child and adolescent psychopathology with ASEBA and SDQ instruments: research findings, applications, and future directions. J Child Psychol Psyc 2008;49(3):251–75. http://dx.doi.org/10.1111/j.1469-7610.2007.01867.x.

Arns M, Peters S. Different brain activation patterns in dyslexic children: evidence from EEG power and coherence patterns for the double-deficit theory of dyslexia. J Integr Neurosci 2007;6(1):175–90. Retrieved from <http://www.worldscientific.com/doi/abs/10.1142/S0219635207001404>.

Bassett DS, Bullmore E. Small-world brain networks. Neuroscientist 2006;12(6):512–23. http://dx.doi.org/10.1177/1073858406293182.

Bastiaansen MCM, Oostenveld R, Jensen O, Hagoort P. I see what you mean: theta power increases are involved in the retrieval of lexical semantic information. Brain Lang 2008;106(1):15–28. http://dx.doi.org/10.1016/j.bandl.2007.10.006.

Blomert L, Vaessen A. 3DM differential diagnostics for dyslexia: cognitive analysis of reading and spelling. Amsterdam, The Netherlands: Boom Test; 2009.

Boersma M, Smit DJ, Boomsma DI, De Geus EJC, Delemarre-van de Waal H, Stam CJ. Growing trees in child brains: graph theoretical analysis of electroencephalography-derived minimum spanning tree in 5- and 7-year-old children reflects brain maturation. Brain Connect 2013;3(1):50–60. http://dx.doi.org/10.1089/brain.2012.0106.

Bullmore E, Sporns O. Complex brain networks: graph theoretical analysis of structural and functional systems. Nat Rev Neurosci 2009;10(3):186–98. http://dx.doi.org/10.1038/nrn2575.

Bullmore E, Sporns O. The economy of brain network organization. Nat Rev Neurosci 2012;13(5):336–49. http://dx.doi.org/10.1038/nrn3214.

Buzsáki G, Draguhn A. Neuronal oscillations in cortical networks. Science 2004;304:1926–30. Retrieved from http://www.sciencemag.org/content/304/5679/1926.short.

de Vos T. Schoolvaardigheidstoets. Amsterdam, The Netherlands: Boom Test; 2007.

Delorme A, Makeig S. EEGLAB: an open source toolbox for analysis of single-trial EEG dynamics including independent component analysis. J Neurosci Meth 2004;134(1):9–21. http://dx.doi.org/10.1016/j.jneumeth.2003.10.009.

Dimitriadis SI, Laskaris NA, Simos P, Micheloyannis S, Fletcher JM, Rezaie R, Papanicolaou AC. Altered temporal correlations in resting-state connectivity fluctuations in children with reading difficulties detected via MEG. NeuroImage 2013;83:307–17. http://dx.doi.org/10.1016/j.neuroimage.2013.06.036.

Finn ES, Shen X, Holahan JM, Scheinost D, Lacadie C, Papademetris X, et al. Disruption of functional networks in dyslexia: a whole-brain, data-driven analysis of connectivity. Biol Psychiatry 2014;76(5):397–404. http://dx.doi.org/10.1016/j.biopsych.2013.08.031.

Fraga González G, Žarić G, Tijms J, Bonte M, Blomert L, van der Molen MW. A randomized controlled trial on the beneficial effects of training letter-speech sound integration on reading fluency in children with dyslexia. PLoS ONE 2015;10(12):e0143914.

Fraschini M, Demuru M, Puligheddu M, Floridia S, Polizzi L, Maleci A, et al. The re-organization of functional brain networks in pharmaco-resistant epileptic patients who respond to VNS. Neurosci Lett 2014;580:153–7. http://dx.doi.org/10.1016/j.neulet.2014.08.010.

Fraschini M, Demuru M, Crobe A, Marrosu F, Stam CJ, Hillebrand A. The effect of epoch length on estimated EEG functional connectivity and brain network organisation. J Neural Eng 2016;13(3):036015.

Frye RE, Liederman J, McGraw Fisher J, Wu M-H. Laterality of temporoparietal causal connectivity during the prestimulus period correlates with phonological decoding task performance in dyslexic and typical readers. Cereb Cortex 2012;22(8):1923–34. http://dx.doi.org/10.1093/cercor/bhr265.

Goswami U. A temporal sampling framework for developmental dyslexia. Trends Cog Sci 2011;15(1):3–10. http://dx.doi.org/10.1016/j.tics.2010.10.001.

Gusnard DA, Raichle ME. Searching for a baseline: functional imaging and the resting human brain. Nat Rev Neurosci 2001;2(10):685–94.

Hampson M, Tokoglu F, Sun Z, Schafer RJ, Skudlarski P, Gore JC, Constable RT. Connectivity-behavior analysis reveals that functional connectivity between left BA39 and Broca's area varies with reading ability. NeuroImage 2006;31(2):513–9. http://dx.doi.org/10.1016/j.neuroimage.2005.12.040.

Klimesch W. EEG alpha and theta oscillations reflect cognitive and memory performance. a review and analysis. Brain Res Rev 1999;29(2-3):169–95. Retrieved from http://www.ncbi.nlm.nih.gov/pubmed/10209231.

Koyama MS, Kelly C, Shehzad Z, Penesetti D, Castellanos FX, Milham MP. Reading networks at rest. Cereb Cortex 2010;20(11):2549–59. http://dx.doi.org/10.1093/cercor/bhq005.

Koyama MS, Di Martino A, Zuo X-N, Kelly C, Mennes M, Jutagir DR, et al. Resting-state functional connectivity indexes reading competence in children and adults. J Neurosci 2011;31(23):8617–24. http://dx.doi.org/10.1523/JNEUROSCI.4865-10.2011.

Koyama MS, Di Martino A, Kelly C, Jutagir DR, Sunshine J, Schwartz SJ, et al. Cortical signatures of dyslexia and remediation: an intrinsic functional connectivity approach. PLoS ONE 2013;8(2):e55454. http://dx.doi.org/10.1371/journal.pone.0055454.

Kruskal JB. On the shortest spanning subtree of a graph and the traveling salesman problem. P Am Math Soc 1956;7(1):48–50.

Lee U, Kim S, Jung K-Y. Classification of epilepsy types through global network analysis of scalp electroencephalograms. Phys Rev E 2006;73(4):041920. http://dx.doi.org/10.1103/PhysRevE.73.041920.

Lee U, Oh G, Kim S, Noh G, Choi B, Mashour GA. Brain networks maintain a scale-free organization across consciousness, anesthesia, and recovery. Anesthesiology 2010;113:1081–91.

Liu K, Shi L, Chen F, Waye MMY, Mok VCT, Chu WCW, Wang D. Altered topological organization of brain structural network in Chinese children with developmental dyslexia. Neurosci Lett 2015;589:169–75. http://dx.doi.org/10.1016/j.neulet.2015.01.037.

Luo H, Poeppel D. Phase patterns of neuronal responses reliably discriminate speech in human auditory cortex. Neuron 2007;54(6):1001–10. http://dx.doi.org/10.1016/j.neuron.2007.06.004.

Marosi E, Harmony T, Becker J. Electroencephalographic coherences discriminate between children with different pedagogical evaluation. Int J Psychopysiol 1995;19:23–32. Retrieved from http://www.sciencedirect.com/science/article/pii/016787609400059N.

Newman MEJ. Mixing patterns in networks. Phys Rev E 2003;67:026126.

Olde Dubbelink KTE, Hillebrand A, Stoffers D, Deijen JB, Twisk JWR, Stam CJ, Berendse HW. Disrupted brain network topology in Parkinson's disease: a longitudinal magnetoencephalography study. Brain 2014;137:197–207. http://dx.doi.org/10.1093/brain/awt316.

Poeppel D, Idsardi WJ, van Wassenhove V. Speech perception at the interface of neurobiology and linguistics. Philos Trans R 2008;363(1493):1071–86. http://dx.doi.org/10.1098/rstb.2007.2160.

Porz S, Kiel M, Lehnertz K. Can spurious indications for phase synchronization due to superimposed signals be avoided? Chaos 2014;24(3):033112. Retrieved from http://scholar.google.com/scholar?hl=en&btnG=Search&q=intitle:No+Title#0.

Pugh KR, Mencl W, Shaywitz B, Shaywitz S, Fulbright RK, Constable RT, et al. The angular gyrus in developmental dyslexia: task-specific differences in functional connectivity within posterior cortex. Psychol Sci 2000;11(1):51–6. Retrieved from http://pss.sagepub.com/content/11/1/51.short.

Quaglino V, Bourdin B, Czternasty G, Vrignaud P, Fall S, Meyer ME, et al. Differences in effective connectivity between dyslexic children and normal readers during a pseudoword reading task: an fMRI study. Clin Neurophysiol 2008;38(2):73–82. http://dx.doi.org/10.1016/j.neucli.2007.12.007.

Raven J, Raven JC, Court JH. Coloured progressive matrices. Oxford, UK: Oxford Psychologists Press; 1998.

Richards TL, Berninger VW. Abnormal fMRI connectivity in children with dyslexia during a phoneme task: before but not after treatment. J Neurolinguist 2008;21(4):294–304. http://dx.doi.org/10.1016/j.jneuroling.2007.07.002.

Sandak R, Mencl W, Frost SJ, Pugh KR. The neurobiological basis of skilled and impaired reading: recent findings and new directions. Sci Stud Read 2004;8(3):273–92.

Schlaggar BL, McCandliss BD. Development of neural systems for reading. Ann Rev Neurosci 2007;30:475–503. http://dx.doi.org/10.1146/annurev.neuro.28.061604.135645.

Schurz M, Wimmer H, Richlan F, Ludersdorfer P, Klackl J, Kronbichler M. Resting-state and task-based functional brain connectivity in developmental dyslexia. Cereb Cortex 2014;25(10):3502.

Shaywitz S, Shaywitz B, Fulbright RK, Skudlarski P, Mencl W, Constable RT, et al. Neural systems for compensation and persistence: young adult outcome of childhood reading disability. Biol Psychiatry 2003;54(1):25–33. http://dx.doi.org/10.1016/S0006-3223(03)01836-X.

Spironelli C, Penolazzi B, Angrilli A. Dysfunctional hemispheric asymmetry of theta and beta EEG activity during linguistic tasks in developmental dyslexia. Biol Psychol 2008;77(2):123–31. http://dx.doi.org/10.1016/j.biopsycho.2007.09.009.

Stam CJ. Modern network science of neurological disorders. Nat Rev Neurosci 2014;15(10):683–95. http://dx.doi.org/10.1038/nrn3801.

Stam CJ, van Straaten ECW. The organization of physiological brain networks. Clin Neurophysiol 2012;123(6):1067–87. http://dx.doi.org/10.1016/j.clinph.2012.01.011.

Stam CJ, Nolte G, Daffertshofer A. Phase lag index: assessment of functional connectivity from multi channel EEG and MEG with diminished bias from common sources. Hum Brain Mapp 2007;28(11):1178–93. http://dx.doi.org/10.1002/hbm.20346.

Stam CJ, Tewarie P, Van Dellen E, van Straaten ECW, Hillebrand A, Van Mieghem P. The trees and the forest: characterization of complex brain networks with minimum spanning trees. Int J Psychophysiol 2014;92(3):129–38. http://dx.doi.org/10.1016/j.ijpsycho.2014.04.001.

Stanberry LI, Richards TL, Berninger VW, Nandy RR, Aylward EH, Maravilla KR, et al. Low-frequency signal changes reflect differences in functional connectivity between good readers and dyslexics during continuous phoneme mapping. Magn Reson Imaging 2006;24(3):217–29. http://dx.doi.org/10.1016/j.mri.2005.12.006.

Tewarie P, Steenwijk MD, Tijms BM, Daams M, Balk LJ, Stam CJ, et al. Disruption of structural and functional networks in long-standing multiple sclerosis. Hum Brain Mapp 2014;35(12):5946–61. http://dx.doi.org/10.1002/hbm.22596.

Tewarie P, Van Dellen E, Hillebrand A, Stam CJ. The minimum spanning tree: an unbiased method for brain network analysis. NeuroImage 2015;104:177–88. http://dx.doi.org/10.1016/j.neuroimage.2014.10.015.

van den Bos KP, Spelberg L, Scheepsma AJM, De Vries JR. De Klepel: Verantwoording, handleiding, Diagnostiek en behandeling. Lisse, The Netherlands: Swets & Zeitlinger; 1999.

van den Heuvel MP, Hulshoff Pol HE. Exploring the brain network: a review on resting-state fMRI functional connectivity. Eur Neuropsychopharm 2010;20(8):519–34. http://dx.doi.org/10.1016/j.euroneuro.2010.03.008.

van der Mark S, Klaver P, Bucher K, Maurer U, Schulz E, Brem S, et al. The left occipitotemporal system in reading: disruption of focal fMRI connectivity to left inferior frontal and inferior parietal language areas in children with dyslexia. NeuroImage 2011;54(3):2426–36. http://dx.doi.org/10.1016/j.neuroimage.2010.10.002.

van Diessen E, Otte WM, Braun KP, Stam CJ, Jansen FE. Does sleep deprivation alter functional EEG networks in children with focal epilepsy? Front Syst Neurosci 2014;8. http://dx.doi.org/10.3389/fnsys.2014.00067.

van Diessen E, Numan T, van Dellen E, van der Kooi AW, Boersma M, Hofman D, et al. Opportunities and methodological challenges in EEG and MEG resting state functional brain network research. Clin Neurophysiol 2015;126(8):1468–81.

van Mieghem P. Performance analysis of complex networks and systems. Cambridge University Press; 2014.

Vandermosten M, Boets B, Wouters J, Ghesquière P. A qualitative and quantitative review of diffusion tensor imaging studies in reading and dyslexia. Neurosci Biobehav R 2012;36(6):1532–52. http://dx.doi.org/10.1016/j.neubiorev.2012.04.002.

Vogel AC, Miezin FM, Petersen SE, Schlaggar BL. The putative visual word form area is functionally connected to the dorsal attention network. Cereb Cortex 2012;22(3):537–49. http://dx.doi.org/10.1093/cercor/bhr100.

Vogel AC, Petersen SE, Schlaggar BL. The VWFA: it's not just for words anymore. Front Hum Neurosci 2014;8:88. http://dx.doi.org/10.3389/fnhum.2014.00088.

von Stein A, Sarnthein J. Different frequencies for different scales of cortical integration: from local gamma to long range alpha/theta synchronization. Int J Psychophysiol 2000;38(3):301–13. Retrieved from http://www.sciencedirect.com/science/article/pii/S0167876000001720.

Vourkas M, Micheloyannis S, Simos P, Rezaie R, Fletcher JM, Cirino PT, Papanicolaou AC. Dynamic task-specific brain network connectivity in children with severe reading difficulties. Neurosci Lett 2011;488(2):123–8. http://dx.doi.org/10.1016/j.neulet.2010.11.013.

Vourkas M, Karakonstantaki E, Simos P, Tsirka V, Antonakakis M, Vamvoukas M, et al. Simple and difficult mathematics in children: a minimum spanning tree EEG network analysis. Neurosci Lett 2014;576:28–33. http://dx.doi.org/10.1016/j.neulet.2014.05.048.

Whitham EM, Pope KJ, Fitzgibbon SP, Lewis T, Clark CR, Loveless S, et al. Scalp electrical recording during paralysis: quantitative evidence that EEG frequencies above 20 Hz are contaminated by EMG. Clin Neurophysiol 2007;118(8):1877–88. http://dx.doi.org/10.1016/j.clinph.2007.04.027.

Wolf RC, Sambataro F, Lohr C, Steinbrink C, Martin C, Vasic N. Functional brain network abnormalities during verbal working memory performance in adolescents and young adults with dyslexia. Neuropsychologia 2010;48(1):309–18. http://dx.doi.org/10.1016/j.neuropsychologia.2009.09.020.

Zhang M, Li J, Chen C, Xue G, Lu Z, Mei L, et al. Resting-state functional connectivity and reading abilities in first and second languages. NeuroImage 2014;84:546–53. http://dx.doi.org/10.1016/j.neuroimage.2013.09.006.